AGU PUBLICATIONS

Water Resources Research

RESEARCH ARTICLE

10.1002/2015WR017296

Benchmarking wide swath altimetry-based river discharge estimation algorithms for the Ganges river system AQ11

Matthew G. Bonnema[1], **Safat Sikder**[1], **Faisal Hossain**[1], **Michael Durand**[2], **Colin J. Gleason**[3], and **David M. Bjerklie**[4] AQ10

[1]Department of Civil and Environmental Engineering, University of Washington, Seattle, Washington, USA, [2]School of Earth Sciences, Ohio State University, Columbus, Ohio, USA, [3]Department of Geography, University of California, Los Angeles, Los Angeles, California, USA, [4]United States Geological Survey, Hartford, Connecticut, USA AQ1

Key Points:
- Effectiveness of three algorithms tested for discharge estimation
- Findings indicate way forward over ungauged basins
- Seasonal changes in flow regime important

Correspondence to:
F. Hossain,
fhossain@uw.edu

Citation:
Bonnema, M. G., S. Sikder, F. Hossain, M. Durand, C. J. Gleason, and D. M. Bjerklie (2016), Benchmarking wide swath altimetry-based river discharge estimation algorithms for the Ganges river system, *Water Resour. Res.*, *52*, doi:10.1002/2015WR017296.

Received 24 MAR 2015
Accepted 7 MAR 2016
Accepted article online 12 MAR 2016

Abstract The objective of this study is to compare the effectiveness of three algorithms that estimate discharge from remotely sensed observables (river width, water surface height, and water surface slope) in anticipation of the forthcoming NASA/CNES Surface Water and Ocean Topography (SWOT) mission. SWOT promises to provide these measurements simultaneously, and the river discharge algorithms included here are designed to work with these data. Two algorithms were built around Manning's equation, the Metropolis Manning (MetroMan) method, and the Mean Flow and Geomorphology (MFG) method, and one approach uses hydraulic geometry to estimate discharge, the at-many-stations hydraulic geometry (AMHG) method. A well-calibrated and ground-truthed hydrodynamic model of the Ganges river system (HEC-RAS) was used as reference for three rivers from the Ganges River Delta: the main stem of Ganges, the Arial-Khan, and the Mohananda Rivers. The high seasonal variability of these rivers due to the Monsoon presented a unique opportunity to thoroughly assess the discharge algorithms in light of typical monsoon regime rivers. It was found that the MFG method provides the most accurate discharge estimations in most cases, with an average relative root-mean-squared error (RRMSE) across all three reaches of 35.5%. It is followed closely by the Metropolis Manning algorithm, with an average RRMSE of 51.5%. However, the MFG method's reliance on knowledge of prior river discharge limits its application on ungauged rivers. In terms of input data requirement at ungauged regions with no prior records, the Metropolis Manning algorithm provides a more practical alternative over a region that is lacking in historical observations as the algorithm requires less ancillary data. The AMHG algorithm, while requiring the least prior river data, provided the least accurate discharge measurements with an average wet and dry season RRMSE of 79.8% and 119.1%, respectively, across all rivers studied. This poor performance is directly traced to poor estimation of AMHG via a remotely sensed proxy, and results improve commensurate with MFG and MetroMan when prior AMHG information is given to the method. Therefore, we cannot recommend use of AMHG without inclusion of this prior information, at least for the studied rivers. The dry season discharge (within-bank flow) was captured well by all methods, while the wet season (floodplain flow) appeared more challenging. The picture that emerges from this study is that a multialgorithm approach may be appropriate during flood inundation periods in Ganges Delta.

1. Introduction

Rivers are among our world's most important natural resources. Nearly every large river on earth is modified by human interactions necessary to sustain society and these modifications have wide reaching impacts on the global water cycle [*Biemans et al.*, 2011; *Pokhrel et al.*, 2012a; *Pokhrel et al.*, 2012b; *Vörösmarty et al.*, 2011] . Rivers provide water for drinking and irrigation to millions of people. The nutrient-rich fertile floodplains that get periodically replenished during floods are essential for round the year crop production. Hydropower generation in run-on-river barrages supplies a significant portion of the world's electricity, and hydropower dam construction is increasing, especially in developing nations [*Zarfl et al.*, 2014]. AQ2

Despite their significance, most of the world's rivers are largely ungauged. Where rivers are gauged, records are available as point-based measurements that do not paint a complete picture of a river system's interaction with the water cycle. Furthermore, the availability of gauged data may be hindered by hydropolitics. In the case of rivers that cross national boundaries, upstream nations can be reluctant to share river gauge data with downstream nations [*Hossain and Katiyar*, 2006]. In situations such as these, remote sensing via satellites is the only available method for obtaining meaningful data from these ungauged rivers [*Alsdorf et al*., 2007; *Schumann et al*., 2009; *Bates*, 2004; *Durand et al*., 2010; *Birkett*, 1998; *Calmant and Seyler*, 2006]. An important parameter for the understanding of surface water dynamics is river discharge. The standard approach to remotely measuring discharge is to extract it from remote sensing observables such as river width, water surface elevation, and water surface slope and apply discharge algorithms that are tailored for such inputs [*Alsdorf et al*., 2007].

Three such algorithms with global applicability are the at-many-stations hydraulic geometry (AMHG) algorithm, the Mean Flow and Geomorphology (MFG) algorithm, and the Metropolis Manning (MetroMan) algorithm. The mechanics of each algorithm are presented in section 3. *Gleason et al*. [2015] recently tested the AMHG algorithm on 34 rivers around the world. They found that under most circumstances, the algorithm discharges had 26%–41% relative root-mean-squared error (RRMSE) agreement with gauged flow rates. However, for braided river conditions and situations where changes in river discharge have a very small effect on river width, the algorithm performs considerably less skillfully with median RRMSE greater than 70% [*Gleason et al*., 2015]. *Gleason and Hamdan* [2016] applied AMHG to the Ganges using Landsat images, and found a dry season RRMSE of 28%, suggesting that the AMHG method could be well suited to the river. *Durand et al*. [2014] has reported 19% RRMSE from the MetroMan algorithm on the River Severn in the UK. Another study found that the Metropolis Manning algorithm overestimates the discharge of the Garonne River [*Berthon et al*., 2014]. There has been no formal test of the MFG algorithm at the time of writing.

The discharge of rivers with high seasonal variability, meandering and braided nature and a tendency to change course, may be more difficult to extract than more stable rivers seen in most places. Such challenging set of river characteristics are often seen in deltas located at the downstream end of large river systems, such as Ganges-Brahmaputra, Nile, Zambesi, Niger, Indus, Salween, and Mekong Rivers. Given the economic and societal importance of most deltas for supporting the food and water needs of large populations, it is important to assess discharge estimation approaches in these locations [*Vörösmarty et al*., 2007, 2009].

Assessment of different discharge estimation methods takes particular importance in this decade as satellite observations on river width and heights are expected to become more widely available. There are currently several concurrently flying nadir altimeters that can measure river heights, such as JASON-1, JASON-2, ENVISAT (this mission ended in May 2012), CryoSat-2, and SARAL/AltiKa. With JASON-2 nearing its phasing out, JASON-3 was launched January 2016. In addition, the first satellite in European Space Agency's (ESA) Sentinel-3 two-satellite constellation launched in February 2016 (Sentinel-3A) and Sentinel-3B will be launched in 2017. The planned Surface Water and Ocean Topography (SWOT) wide swath radar interferometric altimetry mission [*Alsdorf et al*., 2011; *Pavelsky and Durand*, 2012; *Fu et al*., 2012] is scheduled for launch in 2020. Of these planned missions, JASON-3 and Sentinel-3 are actually designated operational missions, dedicated to providing near-real-time data to the general public. Thus, there is an anticipated abundance of satellite water missions that measure height well into the foreseeable future. With such data continuity and declining latency, it is worthwhile to assess discharge algorithms that are amenable to handling remotely sensed inputs of heights, widths, and slope. The first step to this assessment, which is the primary motivation of this study, is to assess the algorithmic (or model-based) uncertainty of each approach. Such a study allows us to understand the various error interactions and provide further guidance on development of discharge estimation methods in preparation of future satellite missions.

Unlike traditional satellite altimeters, which measure elevation at a single point (resulting in a line of elevations measurements as the satellite orbits the earth), the SWOT Mission will provide elevation measurements in wide swaths that allow for the simultaneous measurement of surface water extent and elevation with an observation frequency of 2–3 times within a 21 day period. This unprecedented level of surface water observations will facilitate more robust river discharge estimation algorithms. This study aims to provide a performance comparison of three existing SWOT-based discharge algorithms on the Ganges River delta. It is organized as follows. Section 2 describes the study region and provides a background on the model used to obtain input data for discharge algorithms. Section 3 describes the three algorithms. Section 4 presents a performance comparison between the algorithms. Finally, section 5 summarizes the findings and states the need for future studies to advance satellite-based discharge estimation.

AGU Water Resources Research 10.1002/2015WR017296

2. Study Region, Models, and Data

2.1. Study Region

The region of interest for this study is the Ganges River delta. The massive difference in river flow rates between the wet (Monsoon) and dry seasons makes this region unique for testing the ability of the algorithms to handle large seasonal variability. It is also a water-sensitive delta hosting two mega cities (Kolkata and Dhaka) and the water and food needs of over 200 million people in a changing climate. A majority of the non-Monsoonal flow originates from the Himalayan glaciers and snowpack that sustains the dry season (base) flow and groundwater stocks for water supply and crop production [*Dyurgerov and Meier*, 2005].

Three rivers from the delta region were selected for the study, the Arial-Khan River, Mohananda River, and main stem of the Ganges River. Figure 1 shows the locations of these three rivers within the river system of Bangladesh. The Ganges River was selected for study because it is the major river in this system. The Mohananda and Arial Khan Rivers were selected because they are a tributary and distributary of the Ganges, respectively, and are representative of the many smaller rivers in the delta. These reaches of the Arial Khan and the Mohananda Rivers are single channel, while the Ganges River reach has a few braided sections.

There are some significant differences in the hydraulic characteristics of the selected river reaches. The Ganges River is an order of magnitude wider than the other two rivers studied here. The Arial-Khan River experiences tidal effects which during the dry season causes the river flow direction to reverse during high tides. This behavior is characteristic of delta rivers emptying into an ocean. In spite of their differences, all three rivers experience the sharp change in river flow characteristics during the Monsoon season which is characteristic of most rivers of humid deltas.

2.2. SWOT Mission

The three discharge algorithms tested here (described in section 3) were designed to operate using observations provided by the SWOT mission, scheduled to launch in 2020. This mission will utilize wide swath altimetry to provide spatially distributed water surface elevations. SWOT is expected to provide global observations of rivers larger than 50–100 m, producing significant benefits for global river hydrology [*Pavelsky et al.*, 2014; *Biancamaria et al.*, 2015]. River top width, river surface elevation, and river surface slope, the important variables regarding river discharge, can be derived from these water surface data provided by SWOT. The SWOT mission will produce such observations in 120 km wide swaths, with a 20 km nadir gap (i.e., two 50 km wide swaths on either side of the orbital track, both extending from 10 to 60 km away from nadir). The SWOT satellite will be a polar orbiting satellite with an inclination of 77.6° and a repeat cycle of 21 days (i.e., the satellite will pass over the same location on earth every 21 days). However, because the satellite will observe in a wide swath, most locations on earth will be observed multiple times in one cycle, with higher observational frequency in high latitudes and lower frequency near the equator. The rivers studied here would be observed 2–3 times in one 21 day cycle of the planned SWOT orbit.

2.3. Hydrodynamic Model

Because the SWOT mission will not fly until 2020, a hydrodynamic model of the Ganges delta created with the Hydrologic Engineering Center River Analysis Software (HEC-RAS) was used to simulate the three rivers studied here and to provide the proxy remote sensing variables. This model has been previously calibrated and used for studying satellite river observations of the Ganges delta system [*Sikder and Hossain*, 2014; *Siddique-E-Akbor et al.*, 2014; *Maswood and Hossain*, 2014]. The Manning's roughness parameter at each cross section in the HEC-RAS model (located approximately every 10 km) was previously calibrated based on direct measurements of river height from gauge stations within the delta with boundary conditions specified by upstream gauged discharge and downstream water level. River bathymetry at each cross section was obtained from surveys of the river bed. All modeled cross sections of the Ganges are in locations where the river is single channel. Because of this, the model treats the entire river as single channel. The gauging stations along the selected river reaches are shown as red squares in Figure 2, while the performance of the HEC RAS model on each of these rivers is shown in Figure 3.

Each study reach was subdivided into two or more reaches due to changes in river conditions resulting in significant differences in river hydrodynamics or discharge marked by specific locations. This was done so that the discharge algorithms could be applied to reaches with consistent discharge (i.e., reaches without abrupt changes in discharge or hydrodynamics). For the Ganges and Arial-Khan Rivers, this subdivision was

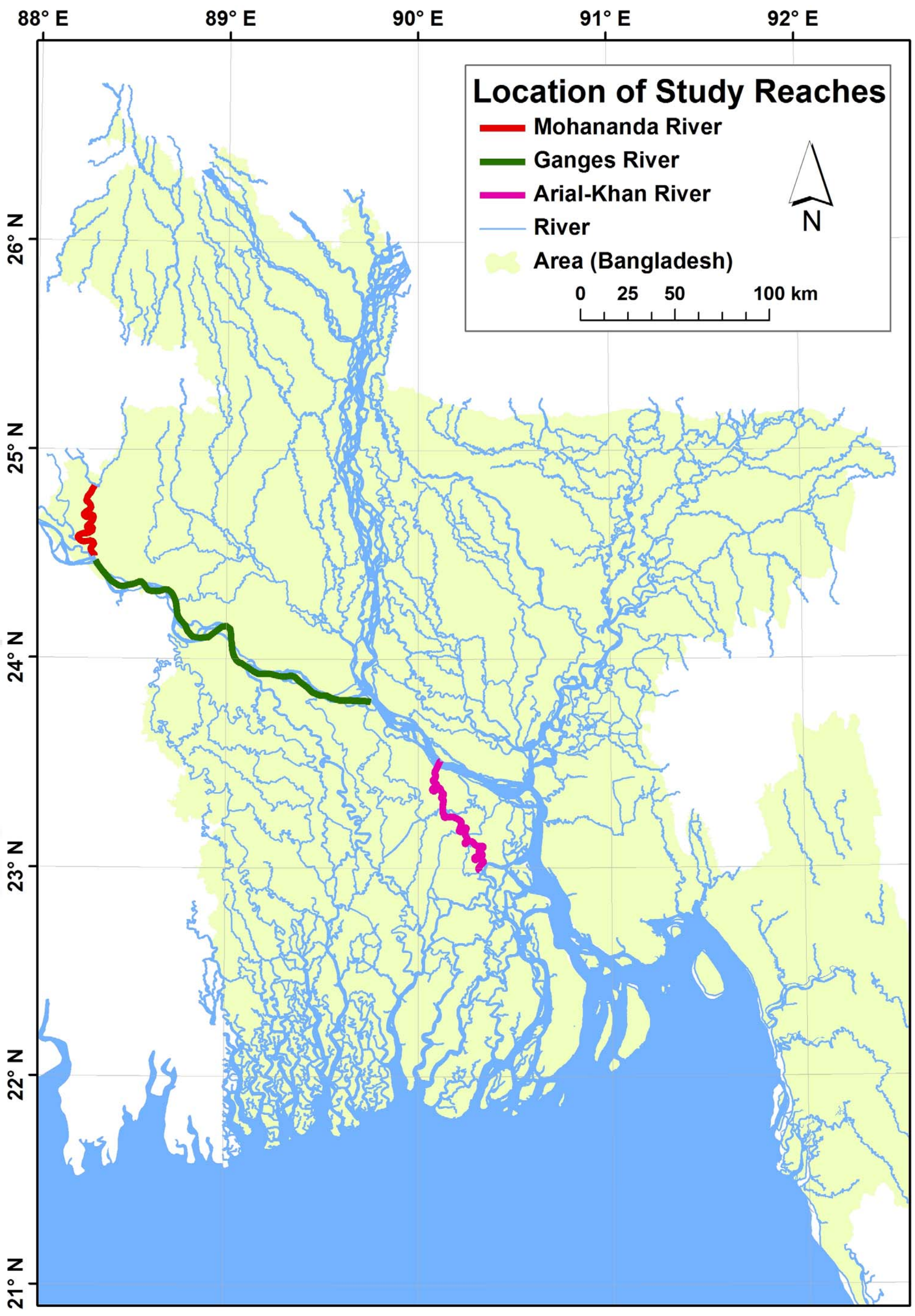

Figure 1. The Ganges Delta showing the selected river reaches that were studied.

determined using the location of tributaries and distributaries along the channel. A sharp change in the slope of the Mohananda River marks the location of its subdivision. These subdivision locations are shown in Figure 4. The length of the resulting reaches ranges from 10 to 100 km. Slope was calculated for each reach segment using the least squares method. These calculated slopes are also depicted in Figure 4. F4

2.4. SWOT Simulator

To gain a better sense of how the algorithms will perform in practical applications with SWOT observations, the SWOT simulator provided by the Jet Propulsion Laboratory (JPL) was used. The required inputs for the

AGU Water Resources Research 10.1002/2015WR017296

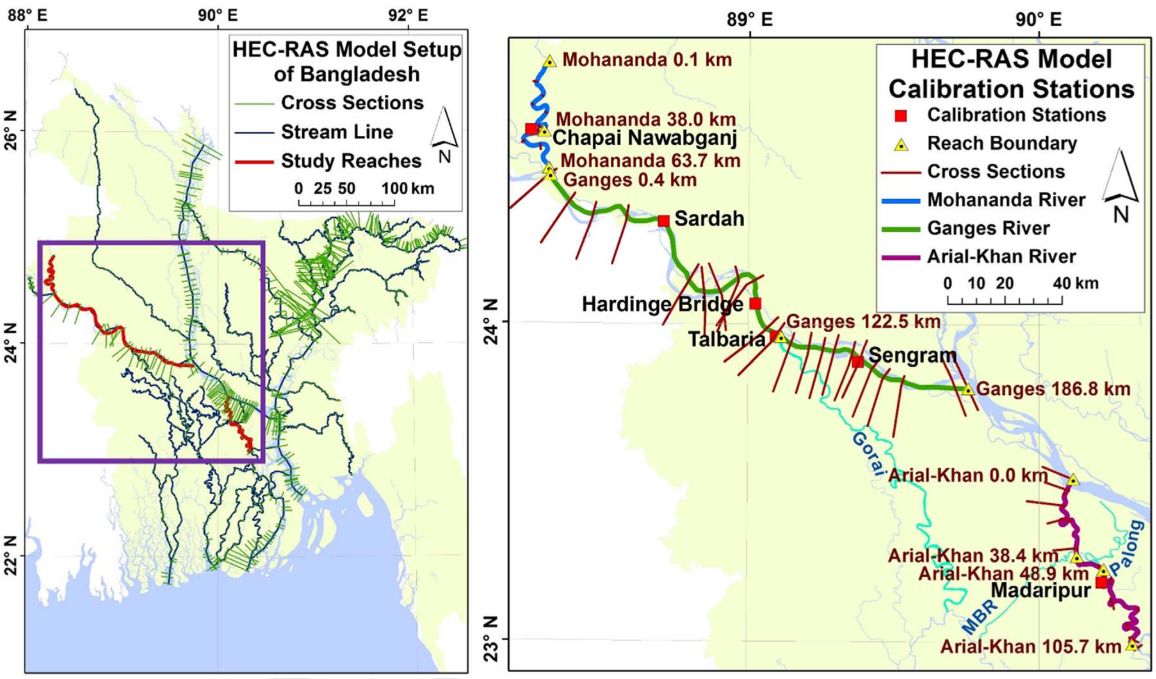

Figure 2. HEC-RAS river hydrodynamic model setup on the Ganges Delta and the calibration station locations within the selected study reaches. The highlighted rivers are study reaches used to delineate reach segments, and the box in the left figure indicates the boundaries of the right figure.

simulator are a water surface elevation layer (typically taken as the "true" water surface) and a DEM (digital elevation model) of the surrounding land surface with river bathymetry. The simulator then applies errors to the water surface elevation according to expected instrument error of the mission, providing a simulation of a SWOT observed water surface. At the time of writing, the SWOT simulator was only equipped to provide errors in river water surface elevation and not river width. The errors included in the simulator were random errors (e.g., instrument inaccuracies), errors caused by signal blockage due to rough topography, and tropospheric errors associated with precipitation.

The SWOT simulator utilizes orbit specifications representative of the mission's planned orbit with a 77.6° inclination, 890 km altitude, and a 21 day repeat cycle. The SWOT mission's planned swath width is 120 km. Here the swath width of the simulator was kept at its default value of 140 km. However, all three river reaches studied here were completely enclosed by the 120 km swath (i.e., no part of the rivers were seen by the additional 20 km provided by the 140 km swath) so for the purposes of this study, the observations generated using the 140 km swath are functionally identical to those that would have been generated using a 120 km swath.

3. Methodology

3.1. Overview

The general methodology behind this study was to first generate river width and water surface elevation data as well as discharge for the three study rivers using the HEC-RAS model of the Ganges delta. Then, use this river width and water surface elevation data as input into each algorithm in a consistent framework and compare the estimated daily discharges with the discharges generated by HEC-RAS model. The 5th, 15th, and 25th of each month from the year 2001 for a total of 36 days were used to assess the performance of each algorithm. This is similar to the sampling frequency expected from the SWOT mission. Daily river data of the entire year 2000 were treated as a priori knowledge and used to calibrate the MFG algorithm parameters (see section 3.5) and provide the prior parameter estimates for the Metropolis Manning algorithm (see section 3.6).

Next, SWOT mission observations were simulated by passing the HEC-RAS model output through the SWOT simulator and use these river observations as inputs into the algorithms to understand how SWOT

AGU Water Resources Research 10.1002/2015WR017296

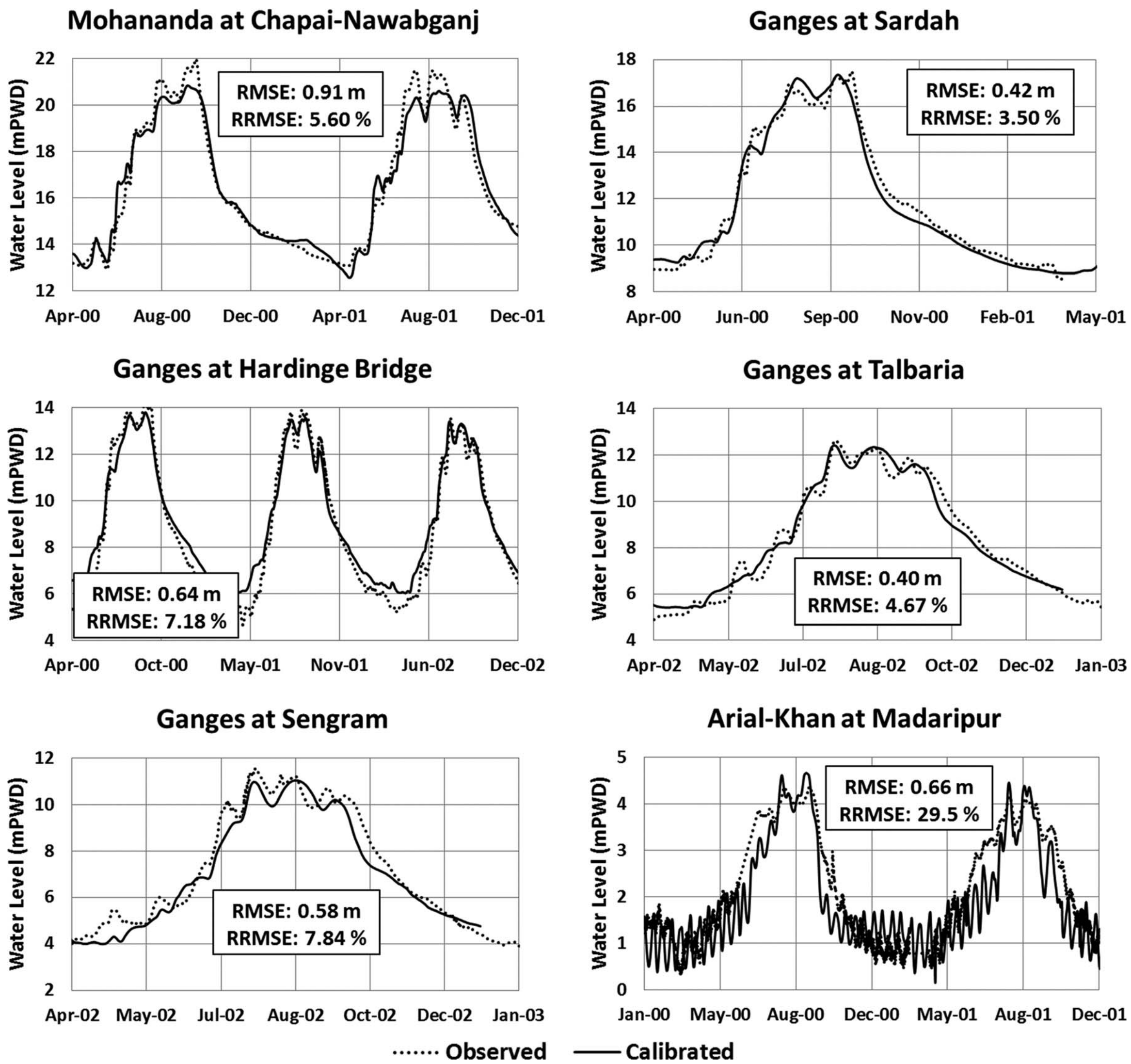

Figure 3. Time series of observed and HEC-RAS simulated water level at gauging stations. Herein RMSE is Root-Mean-Squared Error while RRMSE is the RMSE relative to the average water level and expressed as a %.

uncertainties affect discharge estimation. To help understand how each algorithm works, Figure 5 shows a depiction of an arbitrary river cross section (left) and profile (right) with remote sensing observables of width, depth (above a minimum or reference water depth), and slope.

3.2. Data Processing

In order to derive the river width, water surface elevation, and water slope for use in each algorithm, 10 m resolution water depth rasters were created for the 2000–2001 period using HEC-Geo-RAS [*U.S. Army Corps of Engineers*; *Ackerman*, 2009]. To generate these rasters, first the HEC-RAS model was used to produce river cross sections at 100 m increments using a built in HEC-RAS interpolation tool. These cross sections were imported into GIS from HEC-RAS with the help of HEC-GeoRAS, resulting in 10 m resolution river bathymetry rasters. The generated river bathymetry was merged with 300 m resolution dry land DEMs of the study reaches provided by the Bangladesh Water Development Board (BWDB) and resampled to 10 m. These dry land DEMs were used because their elevations are based off the same local datum, mPWD (meter Public Work Datum), as the HEC-RAS model. Figure 6 shows the 300 m BWDB DEM and the HEC-RAS generated bathymetry (left), as well as the resulting 10 m merged DEM with river bathymetry (right) for the Mohananda River. Next, river depth data output taken from the HEC-RAS model of the study reaches were imported into GIS using HEC-Geo-RAS, resulting in 10 m resolution water depth rasters. These water depth

AGU Water Resources Research 10.1002/2015WR017296

rasters were then merged with the dry land DEMs with river bathymetry to convert them into water surface elevation layers.

River width and height were extracted from the water surface raster by first dividing the raster into 100 m lengths (along river centerline) according to each cells proximity to points on the river centerline corresponding to 100 m increments (i.e., pixels were grouped with their nearest centerline point). River height in each 100 m increment was taken as the average height of all pixels within the 100 m length. River width in each 100 m increment was calculated by dividing the surface area of each increment (number of pixels multiplied by pixel area) by 100 m (the length of the increment). Figure 7 illustrates this data extraction process, from the combination of dry land DEMs with water surface DEMs, to averaging in 100 m increments to generate width, elevation, and slope along the entire reach. River heights and widths were averaged across each increment for each of the selected 36 days of the study period in 2001 for the comparison between algorithms. These reach averaged observations are shown in Figure 8. In this study, it was assumed that the water slope, width, and height data extracted from the water surface DEMs are a perfect representation of actual river conditions.

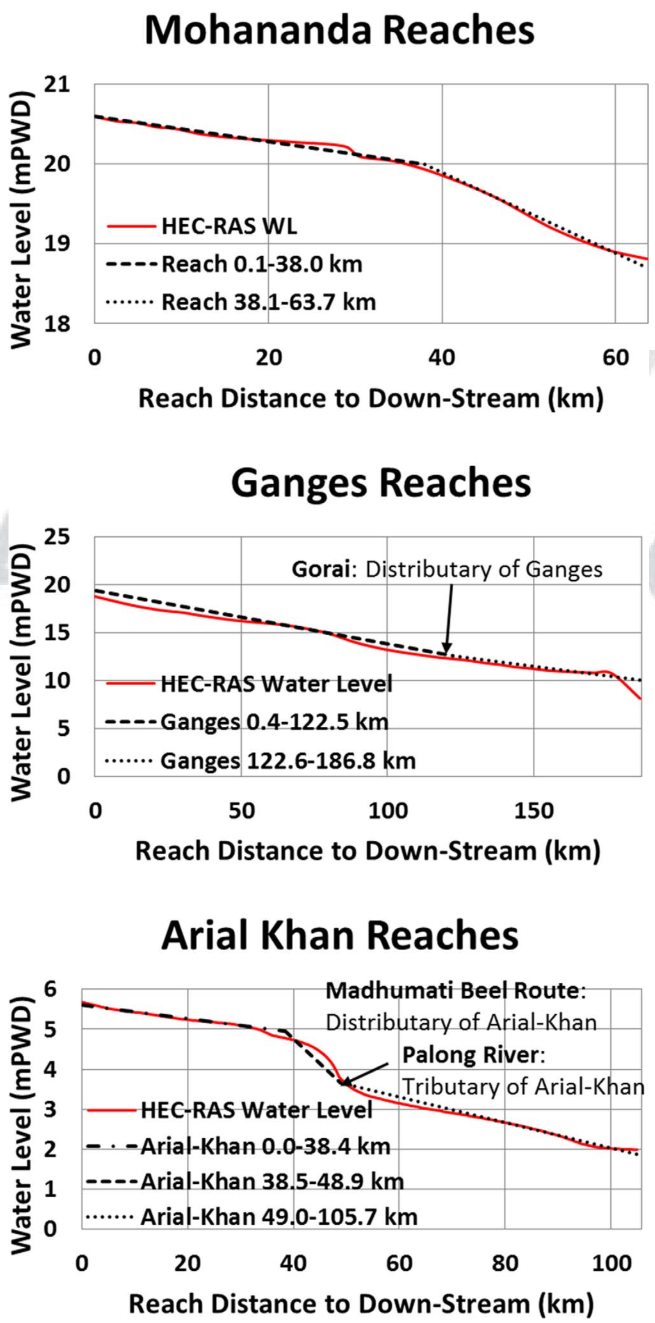

Figure 4. Water level of the Study Reaches on 15 August 2001. This illustrates the slope of each reach and the locations of the reach boundaries.

Preliminary tests of the AMHG method showed that it exhibited inadequate skill when applied over the entire year of the study period in 2001. Because of the high variability of both river width and discharge between the dry and wet seasons and a change in flow regime (within-bank flow versus floodplain flow), we separated the test into two periods: dry season and wet season. To properly compare the performance of the AMHG method to the other two approaches, similar time-period-specific error statistics for the MFG and Metropolis Manning algorithm were calculated. The dry season of 2001 was defined as 5 January through 15 May and the wet season was defined as 25 May through 25 December. Fifteenth May was chosen because in all three rivers, it marks the beginning of sharp increases in flow rate as well as height and width. Shifting this date earlier or later by a few days did not have a significant impact on the results.

3.3. Application of the SWOT Simulator

In order to better understand how the algorithms will perform with real observations, the SWOT simulator was applied in a manner that allowed the exploration of SWOT uncertainty on discharge estimation for Mohananda

AGU Water Resources Research 10.1002/2015WR017296

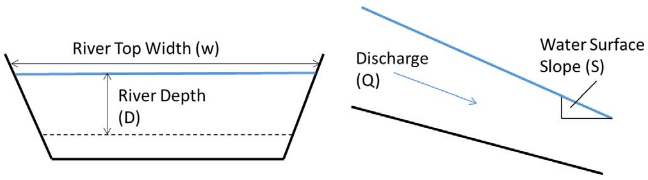

Figure 5. Representation of remote sensing observables of hydraulic features: width, depth, cross-sectional area, and reach averaged slope on a generic cross section.

River. Here river elevation measurements were simulated for each of the 36 days from 2001 using the HEC-RAS generated water depth files. These water heights were averaged within each 100 m long increment and used to determine the slope. The width was taken from the raster file generated from HEC-RAS output, because at the time of writing, estimating river width among SWOT location error had not been well established. No uncertainty was considered for width observations in this study.

The 10 m dry land DEMs with river bathymetry described earlier provided the floodplain topography and river bathymetry needed for the simulator. Additionally, the water surface elevation layers generated from HEC-GeoRAS were used as inputs in to the simulator. The simulator applied random and topographical errors to these water surface elevation layers and created new water surface layers representative of expected SWOT measurements (Figure 9). Since river surface extent could not be extracted from the simulator output, only height errors occurring within the original water surface were considered. Simulated elevation measurements with high vertical error also exhibit high geolocation error, causing them to be located outside the water surface mask. Thus, excluding these points lead to an underestimation of the overall SWOT error. Additionally, it was assumed that no rainfall occurred during SWOT observations and tropospheric errors were neglected.

The SWOT simulator typically runs for a complete cycle of 21 days (i.e., the simulated satellite flies over the same location on the earth every 21 days). Within this cycle, a river reach is expected to be covered at least once by the wide swath of the SWOT orbit. In higher latitudes, the frequency of the coverage will be higher. The Mohananda River reach is entirely covered twice within a cycle by two orbits, once by the right swath of orbit-0261 and again by the left swath of orbit-0498 (Figure 10). The reach is passed by the orbit-0261 and orbit-0498 9.3 and 17.8 days, respectively, from the cycle's starting date. Note that these different orbits result in slightly different simulated water surfaces due to differences in the location of the reach relative to the satellite (e.g., errors at the outer edges of the swath are different than errors at the inner edges of the swath). Here discharge was estimated for both overpasses and averaged.

Sections 3.4–3.6 provide a brief description of each of the discharge estimation approaches.

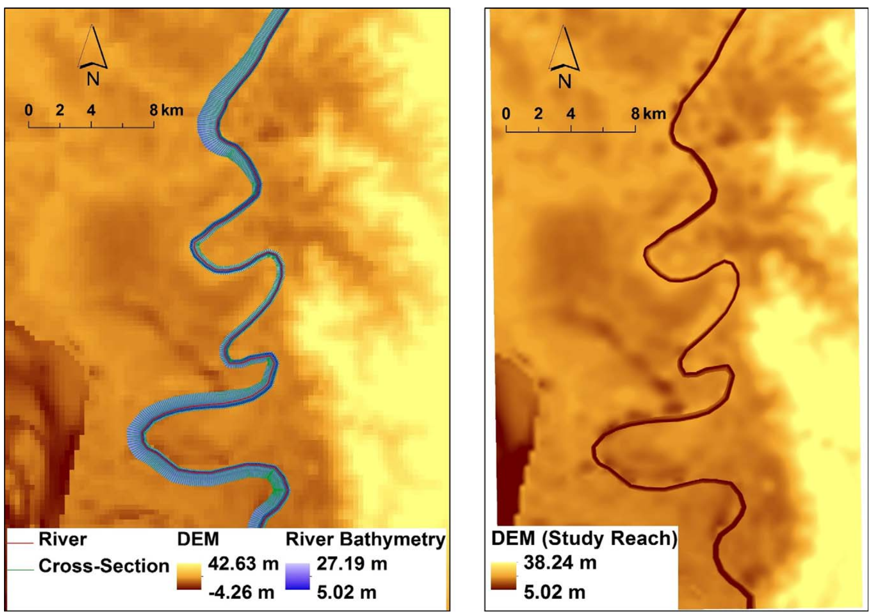

Figure 6. Three hundred meter dry land DEM from the Bangladesh Water Development Board and river bathymetry from HEC-RAS model (left) before merging and (right) 10 m merged dry land DEM with river bathymetry.

AGU Water Resources Research 10.1002/2015WR017296

3.4. At-Many-Stations Hydraulic Geometry (AMHG)

The AMHG algorithm proposed by *Gleason and Smith* [2014] and *Gleason et al*. [2015] is based on the hydraulic geometry relationship between river width (w) and flow rate (Q) given by equation (1), or at-a-station hydraulic geometry (AHG) [*Leopold and Maddock*, 1953]. *Gleason and Hamdan* [2016] have also previously applied this method to the Ganges River using Landsat imagery in a proof-of-concept experiment, finding 28% RRMSE between estimated and observed dry season flows.

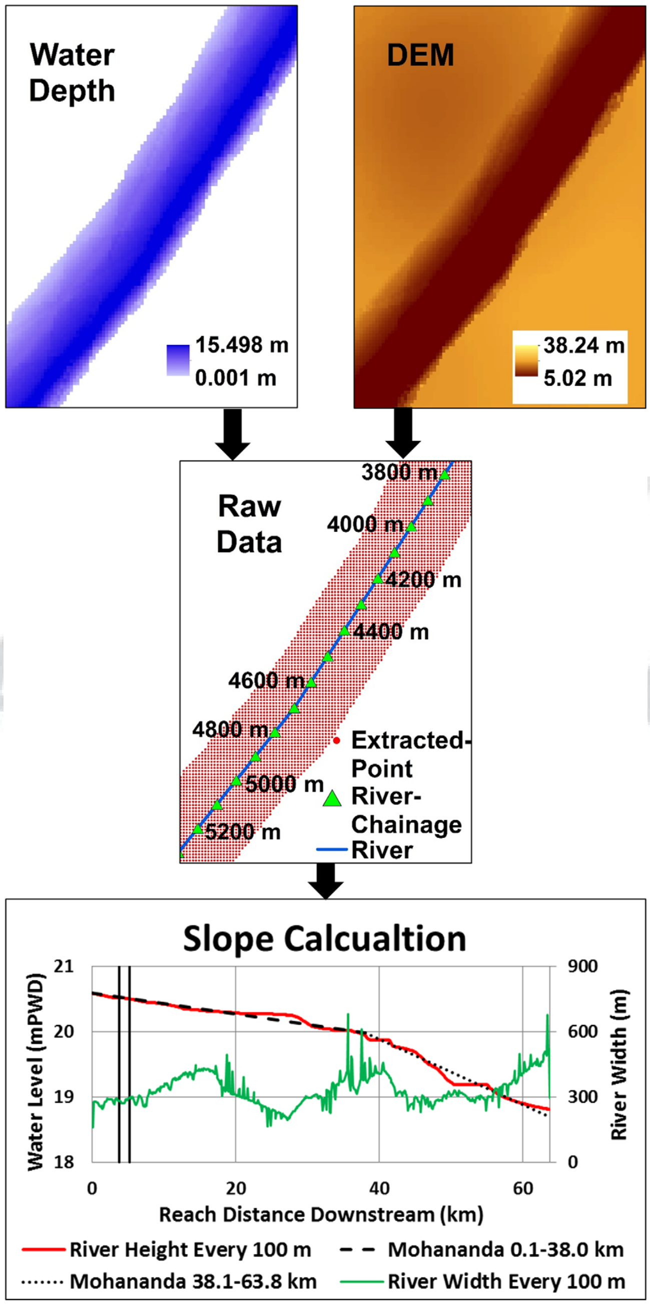

Figure 7. Data processing technique to determine slope of a reach and river width. The "DEM" in the top right figure represents the dry land (without water) elevation model. (top left) This DEM was merged with the water depth layer to generate the (middle) water elevation layer. (bottom) From the water surface elevation layer, width, elevation, and slope were extracted. The black vertical lines in the bottom figure show the location along the reach of the data shown in the top and middle figures. Elevation of water surface is relative to a local datum called meter Public Water Datum (mPWD) which is about 0.45 m above local mean sea level.

$$w = aQ^b \tag{1}$$

where

w = width of river surface at any cross section at any point in time;

Q = river discharge;

a and b = hydraulic geometry parameters.

The a and b terms are hydraulic geometry parameters which are unique to each cross section along a river. *Gleason and Smith* [2014] first showed that a previously unknown relationship between a and b parameters existed, and termed this relationship as AMHG, equation (2).

$$b = -AMHG \times \log(a) + AMHG \times \log(w_{glob}) \tag{2}$$

where

w_{glob} = mean of all observed widths in a study reach over space and time;

$AMHG$ = slope of the $b - \log(a)$ relationship;

a and b = hydraulic geometry parameters.

AMHG thus relates cross-sectional AHG parameters in space. A proxy for the slope of a river's AMHG which only requires repeated width measurements of the river reach, given by equation (3), has been used to determine AMHG in the past.

$$\log(\max(w_{x1,x2,\ldots xn})) = \frac{1}{AMHG}\log\left(\max(w_{x1,x2,\ldots xn})^2 - \min(w_{x1,x2,\ldots xn})^2\right) + p \tag{3}$$

where

$AMHG$ = slope of the $b - \log(a)$ relationship;

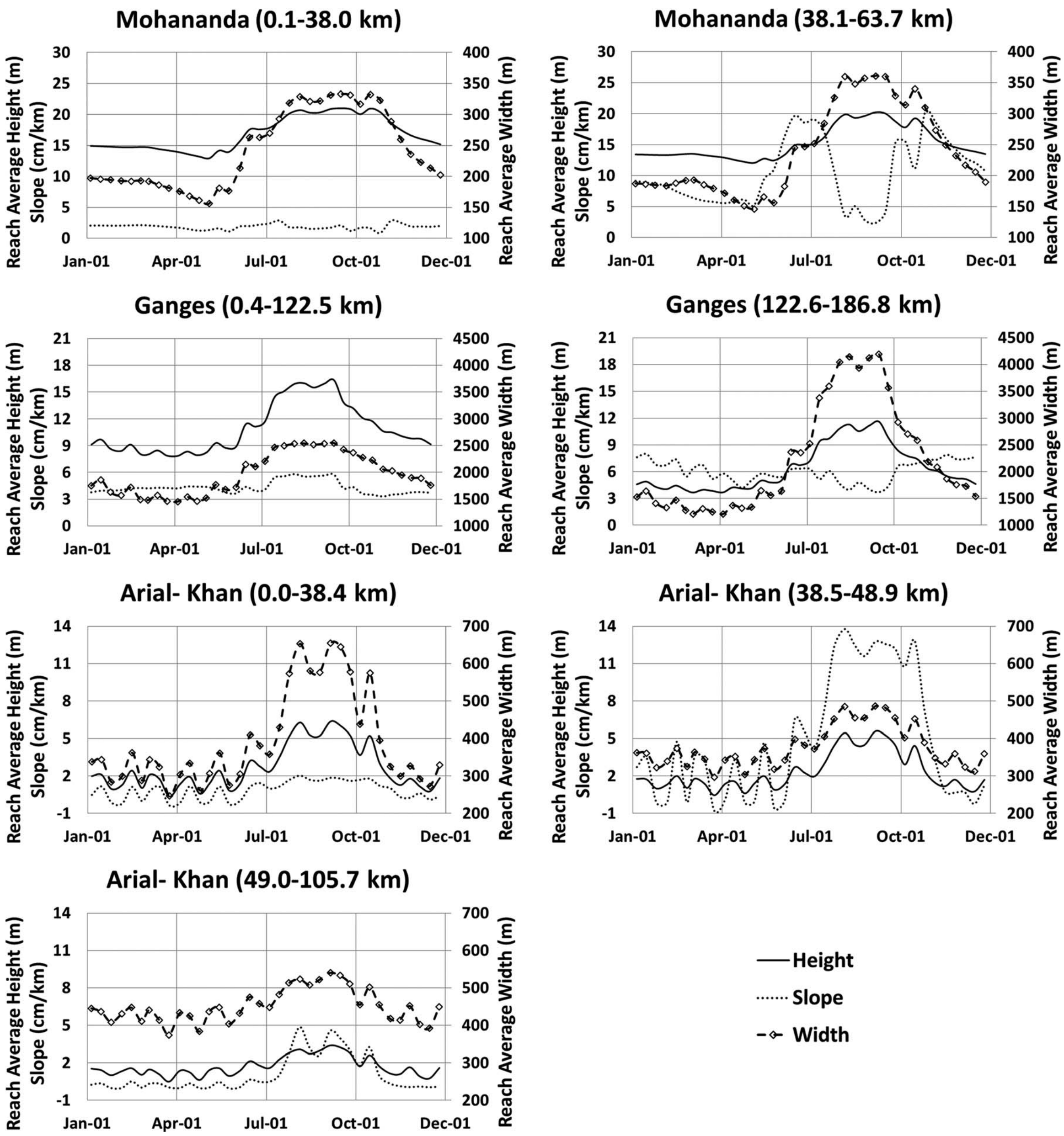

Figure 8. Reach averaged water surface height, width, and slope (slope is positive at downward direction) of study reaches for 36 days of the independent validation period in 2001.

$w_{x1,x2,...xn}$ = width of river corresponding to each cross section of the reach;

p = empirical regression parameter.

This relationship is not guaranteed to perfectly predict a river's AMHG. *Gleason and Wang* [2015] found this relationship to be unreliable, however, it is assumed to apply to the rivers studied here. An exploration of the impact of using this proxy on discharge estimation is presented in section 4.4.

Using equation (3), the AMHG can be calculated for a given reach via linear regression, allowing the relationship between a cross section's a and b to be known. The p term represents the intercept of the linear regression and is not used in determining the AMHG. Next, an optimization routine (in this case, a genetic algorithm [*Gleason and Smith*, 2014]) is used to determine the a and b parameters for each cross section in the river reach by minimizing the difference in flow rates between each cross section. The optimization routine is constrained in its search by AMHG and by discharge constraints proposed by *Gleason and Smith*

AGU Water Resources Research 10.1002/2015WR017296

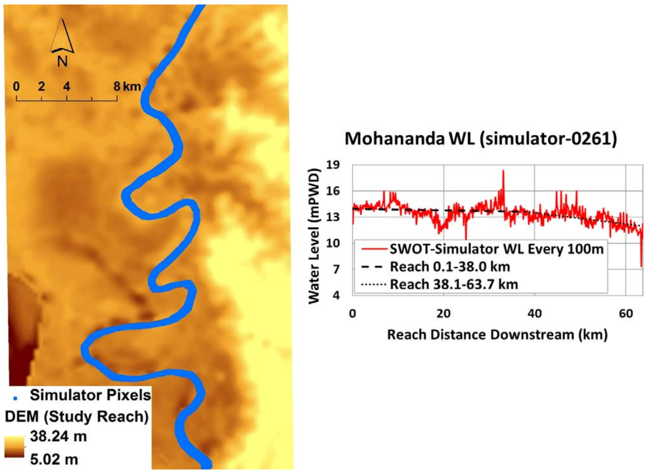

Figure 9. Application of the SWOT simulator. (left) Water surface elevation raster generated by the SWOT simulator; (right) averaged SWOT simulator WL at each 100 m increment of the Mohananda River on 15 April 2001 (orbit-0261).

[2014]. The genetic algorithm is here run 50 times for 50 generations each, with random start points and an average of all the resulting flow rates is output as the river reach's discharge. The results were insensitive to the number of genetic algorithm runs (this is consistent with the sensitivity analysis performed in *Gleason et al.* [2015]) and 50 runs of 50 generations were used, because this matched the procedure used in *Gleason and Smith* [2014]. Figure 11 shows a flowchart breakdown of the implementation of the AMHG algorithm.

A brief sensitivity analysis was performed to determine the sensitivity of the AMHG method to the number of cross sections used to calculate discharge. It was found that the method was insensitive to this parameter as long as more than 15 cross sections were used. In this study, we used 25 equally spaced cross sections for each reach to balance the 15 cross section limit found in the sensitivity analysis while maintaining fewer cross sections to achieve reasonable computation speed. The water surface widths at these cross sections were taken from the 10 m water surface DEM generated from HEC-GeoRAS.

3.5. Mean Flow and Geomorphology Algorithm

The MFG algorithm is developed from conceptual approaches discussed in *Bjerklie et al.* [2003, 2005] and *Dingman and Bjerklie* [2005]. The algorithm assumes a mean value for the Manning friction coefficient that is modified based on the change in cross-sectional flow area, assumes a regular geometric shape for the cross section such that the change in maximum depth measured by change in stage can be translated into

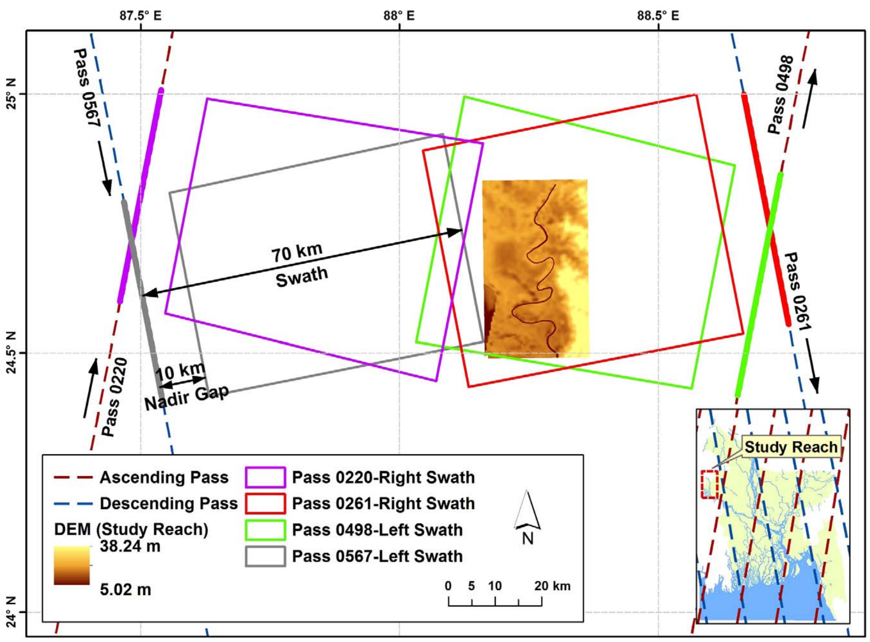

Figure 10. SWOT orbital pass and coverage over the Mohananda River reach. The lower right figure in the inset shows the SWOT coverage with a 21 day repeat cycle at 77.6° inclination.

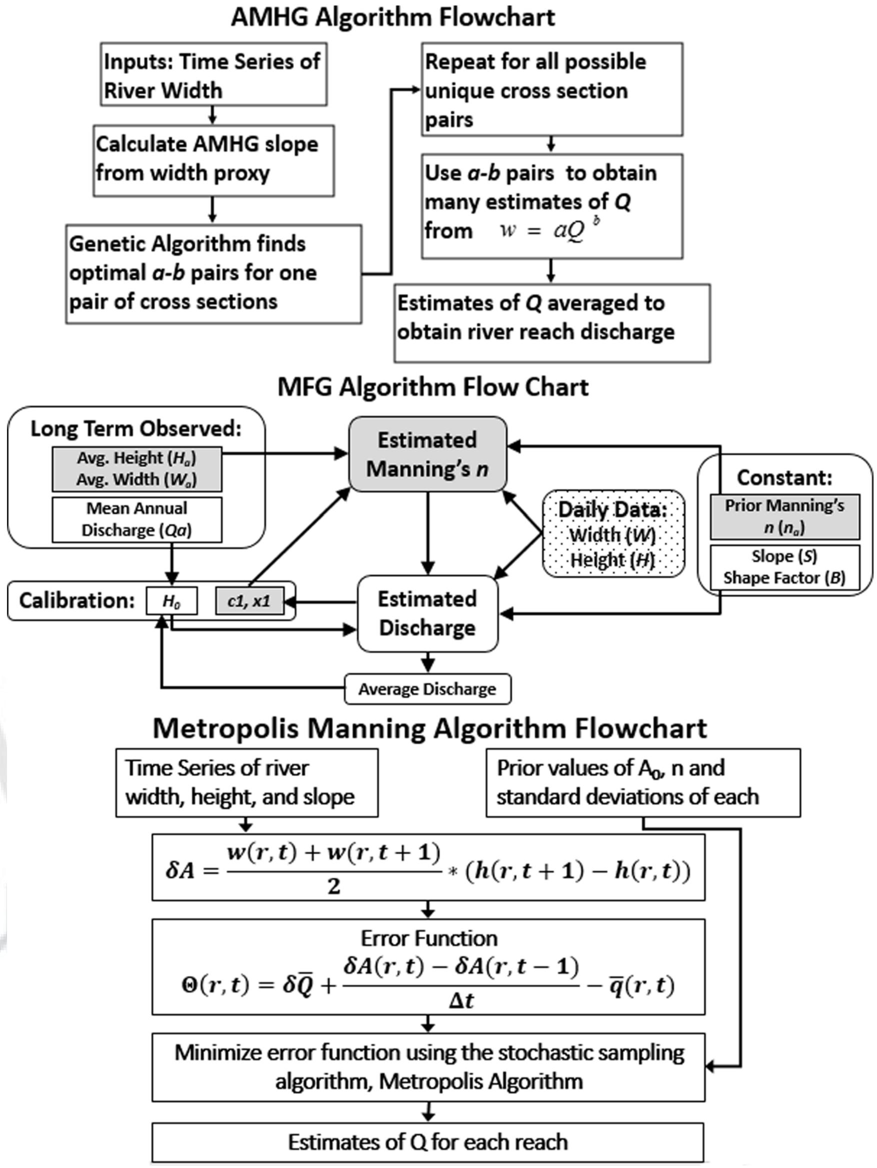

Figure 11. Flowchart of steps to calculate discharge using (top) the AMHG algorithm, (middle) the MFG algorithm, and (bottom) the Metropolis Manning algorithm.

the change in the mean flow depth of the cross section, and assumes a minimum or zero flow stage. The general relation is given in equation (4).

$$Q = \frac{1}{n}\left([H - H_o]Y^*\right)^{\frac{5}{3}} W S^{\frac{1}{2}} \tag{4}$$

where

n = estimated Manning's resistance coefficient;

W = observed width;

H = observed height;

S = mean slope of the river (water surface assuming equivalent to energy slope);

Y^* = fraction to derive mean cross section depth, $1 - \frac{1}{1+B}$, and B is the shape factor (2 for parabolic cross section and 10 for Rectangular cross section);

AGU Water Resources Research 10.1002/2015WR017296

H_o = the zero flow depth which is individually calibrated with mean annual flow.

The mean water surface slope was derived from the HEC-RAS model output for the year 2000. A rectangular cross section was assumed in calculating Y* (with B equal to 10).

The Manning's *n* value is assumed to be associated with the mean value of channel width and stage. This Manning's *n* value is varied according to the change in channel cross section as indexed by equation (5).

$$n = c1\left(\frac{WH}{W_a H_a}\right)^{x1} n_a \quad (5)$$

where,

W_a = long-term average of observed width;

H_a = long-term average of observed height;

n_a = input average Manning's n.

The long-term width and height observations were taken from the daily output from the HEC-RAS model for the year 2000. The input average Manning's n used here was 0.025. Section 4.5 shows that this method is relatively insensitive to the Manning roughness input. The coefficients, $c1$ and $x1$, remain constant through time and were calibrated based on daily water surface elevation and mean annual discharge from the same HEC-RAS model output for the year 2000. While an entire year of daily data was used here, the calibration of these coefficients can proceed using limited time series of stage or general relationships developed on rivers in a similar setting and then further calibration can be performed as more satellite observations become available. For the three rivers studied here, the difference between annual average height, width, slope, and discharge calculated from daily values and calculated from a more limited time series (the 5th, 15th, and 25th of each month) were less than 0.1%, ultimately leading to no difference in discharge estimation. It is anticipated that initial empirically derived default values for *B*, na, $c1$, and $x1$ can be optimized over time based on validation time series, and improved understanding of the relation between the coefficient values and river characteristics.

The value for the minimum flow depth H_0 is optimized by calibrating the time series of observed width, stage, and slope to the mean discharge for the river, and as such is dependent on knowledge of the mean discharge. It is assumed that the mean discharge is available from various global databases, or from global circulation and hydrologic models, or from other sources.

The parameterization of Manning's *n* cannot address tidal flux, because in these environments, the relation between change in Manning's *n* and change in cross section does not necessarily have any validity. This is because the flow resistance is dominated by backwater effects and varies substantially during periods of adverse (upstream) slope (incoming flood tide) and downstream slope (outgoing ebb tide). However, a modified relation between cross-sectional change and slope could be developed to account for this deficiency.

The MFG algorithm relies on the prior estimation of average Manning's n (n_a) and mean annual flow to calibrate the H_o. The sensitivity of the algorithm to prior estimations of these parameters is explored in section 4.5. This discharge estimation algorithm can be applied to calculate cross-sectional discharge as well as reach averaged discharge. In this study, reach averaged observations were used for this method resulting in reach averaged discharge. Figure 11 shows the algorithm structure for calibrating $c1$, $x1$, and H_0 and estimating discharge.

3.6. Metropolis Manning Algorithm

The Metropolis Manning algorithm also uses a form of Manning's equation paired with mass conservation as a basis for determining discharge [*Durand et al.*, 2014]. Equation (6) shows Manning's equation as used by this algorithm. Note that the bar signifies reach averaged quantities.

$$\bar{Q}(r,t) = \frac{1}{n(r)}\left[\bar{A}_0(r) + \delta\bar{A}(r,t)\right]^{5/3} w(r,t)^{-2/3} \bar{S}(r,t)^{1/2} \quad (6)$$

where

AGU Water Resources Research 10.1002/2015WR017296

r = denotes reach;

t = denotes time step;

n = Manning's n;

A_0 = base flow area;

δA = deviation in flow area from base flow area;

w = river top width;

S = river slope;

Q = discharge.

Equation (7) gives the mass conservation of the river.

$$\frac{\partial \bar{Q}}{\partial x}(r,t)+\frac{\partial \bar{A}}{\partial t}(r,t)=\bar{q}(r,t) \tag{7}$$

where

$\frac{\partial \bar{Q}}{\partial x}$ = partial derivative of flow rate with respect to the downstream direction;

$\frac{\partial \bar{A}}{\partial t}$ = partial derivative of flow area with respect to time;

$\bar{q}$ = reach averaged lateral inflows.

Discretizing equation (7) between two remote sensing overpasses gives equation (8). By minimizing equation (8), the optimal Manning's n and base flow area can be obtained.

$$\Theta(r,t)=\delta_{r,t}\bar{Q}_{r,t}+\frac{\delta\bar{A}(r,t)-\delta\bar{A}(r,t-1)}{\Delta t}-\bar{q}(r,t) \tag{8}$$

where

$\Theta(r,t)$ = error for reach r at time t;

$\delta_{r,t}$ = constant dependent on length of reach, see *Durand et al*. [2014] for more details.

The error term in equation (8) is minimized using a stochastic sampling algorithm known as the Metropolis algorithm that uses a Bayesian probability updating scheme to create a Markov chain of the unknown parameters, n and A_0. The Markov chain is run for 100,000 iterations and the end result is likely values for the Manning's n and base flow area. With these parameters known, equation (6) is solved to provide discharge.

In this study, lateral inflow (q) was assumed to be 0. This is valid for the synthetic experiment in this study, because the HEC-RAS model does not take into account smaller tributaries, distributaries, or groundwater effects. In application, this assumption would likely decrease the accuracy of this method. The prior base flow area (A_0) was estimated using minimum river width and discharge from the year 2000 calibration data set and assuming a water depth of 1 m. The standard deviation of this base flow area estimate was set as 20% of the base flow area estimate. The initial estimate of Manning's n was taken as 0.025 with a standard deviation of 0.01. The standard deviation of slope, height, and width for all reaches were defined as 0.5 cm/km, 1 cm, and 1 m, respectively. These values represent the uncertainty in the observations. To test the algorithmic uncertainty of the Metropolis Manning algorithm, the observations are assumed to be perfect. However, this algorithm requires these values to be nonzero. For this reason, relatively small standard deviations of the observations were selected.

This algorithm was designed to operate using more than three river reaches. Here the study reaches were discretized further, similar to the manner *Durand et al*. [2014] further discretized their study reach of the River Severn. In this past study, river subreaches ranged from 6.7 to 8.2 km. Here we partitioned each study reach in an attempt to match the reach length used in *Durand et al*. [2014]. However, this was balanced against the increasing computational expense caused by increasing the number of reaches. The Ganges was split into nine subreaches (each approximately 20 km in length), the Mohananda was split into six subreaches (each approximately 10 km in length), and the Arial-Khan was split into five subreaches (each

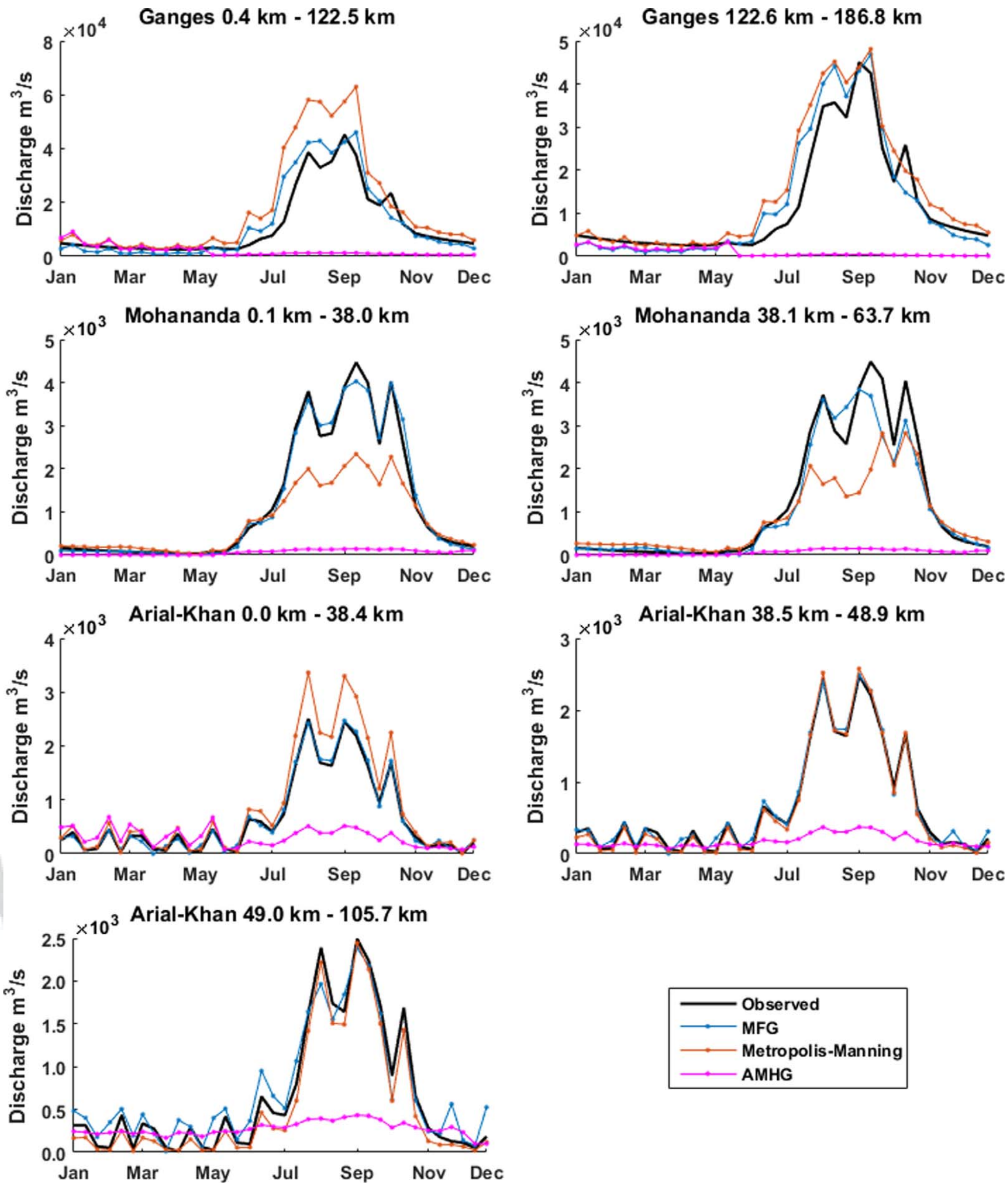

Figure 12. Comparison of performance of each algorithm on the Ganges, Mohananda, and Arial-Khan Rivers during the independent validation period of 2001.

approximately 20 km in length). All subreaches maintained the 100 m spacing between width and height observations described in section 3.2. Since this algorithm provides reach averaged discharge, length weighted average discharges were calculated which correspond to the original study reaches defined in section 2 for comparison to the other two algorithms.

4. Results

4.1. Ganges River Results

Figure 12 shows the reach averaged discharge estimated by the discharge algorithms on the two sub- F12 reaches of the Ganges River and Table 1 provides root-mean-squared error (RMSE), relative root-mean- T1 squared error (RRMSE), bias, and percentage of error that is bias for each algorithm. The RRMSE is the RMSE relative to the average observed discharge (from HEC-RAS model) and expressed as a %. All three algorithms provided satisfactory results during the dry season (48%–54% RRMSE) for the first reach

Table 1. Error Statistics of the Discharge Algorithms for Ganges River During the Study Period of 2001

	MFG		Metropolis Manning		AMHG	
	Dry	Wet	Dry	Wet	Dry	Wet
Ganges 0.4–122.5 km						
RMSE (m^3/s)	1,592	5,741	1,745	13,159	1,779	20,530
RRMSE (%)	48.4	34.4	53.1	78.8	54.1	122.9
Bias (m^3/s)	1,542	2,191	1,110	9,387	812	15,244
% of error from bias	96.8	38.2	63.6	71.3	45.6	74.3
Ganges 122.6–186.8 km						
RMSE (m^3/s)	1,574	5,384	589	6,998	1,310	21,217
RRMSE (%)	47.8	32.2	17.9	42.0	39.8	126.8
Bias (m^3/s)	1,594	1,961	137	4,890	1,307	15,566
% of error from bias	97.7	36.6	23.2	69.9	96.2	73.5

(0.4–122.5 km). The Metropolis Manning algorithm showed much greater accuracy on the dry season of the second reach (17.9% RRMSE) with the other two algorithms showing performance similar to their first reach performance. The AMHG algorithm significantly reduces in skill during the wet season when compared to the other two algorithms. This is in contrast to previous application of AMHG in the basin, as *Gleason and Hamdan* [2016] used Landsat imagery to demonstrate AMHG for the Ganges near Hardinge Bridge, and they found an RRMSE of 28% for dry season flows when compared to discharge measured on the same day as the Landsat images. However, a difference is expected because *Gleason and Hamdan* [2016] used real observations and assumed an AMHG parameter that matched with observations. The Metropolis Manning algorithm also showed a decrease in accuracy during the wet season on both reaches which corresponds to an increase in error associated with bias. The MFG algorithm performed better in the wet season than the dry season with 10%–15% lower RRMSE. This increase in performance is accompanied by a large decrease in the error associated with bias. Overall, the MFG algorithm outperforms the Metropolis Manning and AMHG algorithms in the wet season, while each algorithm appears to perform well in the dry season.

4.2. Mohananda River Results

Figure 12 shows the results of the discharge algorithms on the two subreaches of the Mohananda River and Table 2 provides RMSE and RRMSE for each algorithm. The MFG algorithm showed skill in both seasons, T2 with better performance in the wet season than the dry season. The Manning Metropolis algorithm also performed better in the wet season than the dry season, but the extracted discharge estimates were much worse than those of the MFG algorithm. A large percentage of the Metropolis Manning's error during the dry season was associated with bias. The AMHG was unable to extract skillful discharge estimates during both dry and wet seasons for both river segments. A possible cause of this is the inability of the width proxy to accurately estimate the Mohananda River's AMHG parameter for both dry and wet seasons. This idea is explored further later in this section. The MFG algorithm shows a clear performance advantage over the other two algorithms on the Mohananda River.

4.3. Arial Khan River Results

Figure 12 shows the results of the discharge algorithms on the three subreaches of the Arial Khan River and Table 3 provides RMSE and RRMSE for each algorithm. It is important to note that the AMHG and MFG T3

Table 2. Error Statistics of the Discharge Algorithms for Mohananda River During the Study Period of 2001

	MFG		Metropolis Manning		AMHG	
	Dry	Wet	Dry	Wet	Dry	Wet
Mohananda 0.1–38.0 km						
RMSE (m^3/s)	29	197	66	1049	90	2412
RRMSE (%)	35.9	10.5	81.7	55.9	110.8	128.5
Bias (m^3/s)	19	6	58	644	80	1702
% of error from bias	66.5	3.1	88.2	61.4	89.2	74.0
Mohananda 38.1–63.7 km						
RMSE (m^3/s)	47	480	119	1034.7	90	2406
RRMSE (%)	58.0	25.6	146.0	55.2	109.7	128.4
Bias (m^3/s)	19	192	116	570	80	1697
% of error from bias	39.7	39.9	97.0	55.1	89.6	74.0

Table 3. Error Statistics of the Discharge Algorithms for Arial Khan River During the Validation Period of 2001

	MFG		Metropolis Manning		AMHG	
	Dry	Wet	Dry	Wet	Dry	Wet
Arial-Khan 0.0–38.4 km						
RMSE (m^3/s)	64	64	75	408	187	957
RRMSE (%)	29.7	6.9	35.0	43.9	86.8	102.8
Bias (m^3/s)	7	18	57	288	170	639
% of error from bias	10.4	27.8	75.2	70.7	90.7	66.8
Arial-Khan 38.51–48.9 km						
RMSE (m^3/s)	86	68	60	54	168	1072
RRMSE (%)	42.2	7.3	29.4	5.8	82.1	115.0
Bias (m^3/s)	23	24	49	22	74	700
% of error from bias	26.1	35.4	81.1	41.2	43.8	68.5
Arial-Khan 49.0–105.7 km						
RMSE (m^3/s)	182	215	114	163	146	1023
RRMSE (%)	94.5	23.0	58.9	17.5	75.7	109.6
Bias (m^3/s)	125	37	80	144	46	610
% of error from bias	68.4	17.2	70.6	88.3	31.6	62.5

algorithms are unable to vectorize flow as Metropolis Manning algorithm (positive flow is flow along the downstream direction; negative flow is flow in the upstream direction), but should still properly capture the magnitude of the flow when a river switches flow direction. The output of these two algorithms were therefore compared with the absolute value of the observed discharge for a more accurate error analysis during the dry season with heavy tidal effects (i.e., during high tide). This is realistic because while the algorithms themselves have no method of determining flow direction, it can easily be determined form SWOT observations of river slope. Figure 12 shows the absolute value of the observed discharge and the absolute value of the Manning Metropolis estimated discharge to show a fairer comparison between each algorithm output.

For all three reaches of the Arial-Khan River, both the MFG and Metropolis Manning algorithms showed high skill during the wet season (6.9%–23.0% RRMSE). Dry season discharge estimation was more challenging for all three approaches than wet season, possibly due to the high tidal effects on the river causing diurnal change in flow regime from within bank to floodplain flow quite frequently. The Metropolis Manning algorithm was the only one to consistently provide accurate discharge estimations during the dry season. The Metropolis Manning algorithm showed high error associated with bias while the MFG algorithm's error showed less bias. Once again, the AMHG algorithm failed to produce skillful discharge estimates, possibly caused by the method's width proxy inaccurately estimating the AMHG parameter.

4.4. Improving the AMHG Algorithm

To better understand where the large errors from the AMHG may be originating from, estimation of the AMHG slope was examined via the width proxy. The AMHG for each river for the year 2001 for both dry and

Table 4. Comparison Between Proxy AMHG and Observed "True" AMHG

River	Reach (km)	Directly Calculated AMHG	Direct AMHG R^2	Proxy Estimated AMHG	% Difference Between Proxy and Direct
Ganges Dry	0.4–122.5	−0.1189	0.99	−0.0901	27.6
	122.6–186.8	−0.1208	0.97	−0.4502	115.4
Ganges Wet	0.4–122.5	−0.0965	0.99	−0.4157	124.6
	122.6–186.8	−0.1052	0.93	−0.2725	88.6
Arial-Khan Dry	0.0–38.4	−0.1095	0.88	−0.2793	87.3
	38.5–48.9	−0.0244	0.04	−0.3141	171.2
	48.9–105.7	−0.0108	0.04	−0.2377	182.6
Arial-Khan Wet	0.0–38.4	−0.1540	0.96	−0.3712	82.7
	38.5–48.9	−0.0449	0.30	−0.0484	7.5
	48.9–105.7	−0.0665	0.56	−0.2708	121.1
Mohananda Dry	0.1–38.0	−0.0883	0.71	−0.4958	139.5
	38.1–63.7	−0.1207	0.68	−0.3741	102.4
Mohananda Wet	0.1–38.0	−0.1048	0.83	−0.4134	119.1
	38.1–63.7	−0.1302	0.89	−0.4081	103.3

AGU Water Resources Research 10.1002/2015WR017296

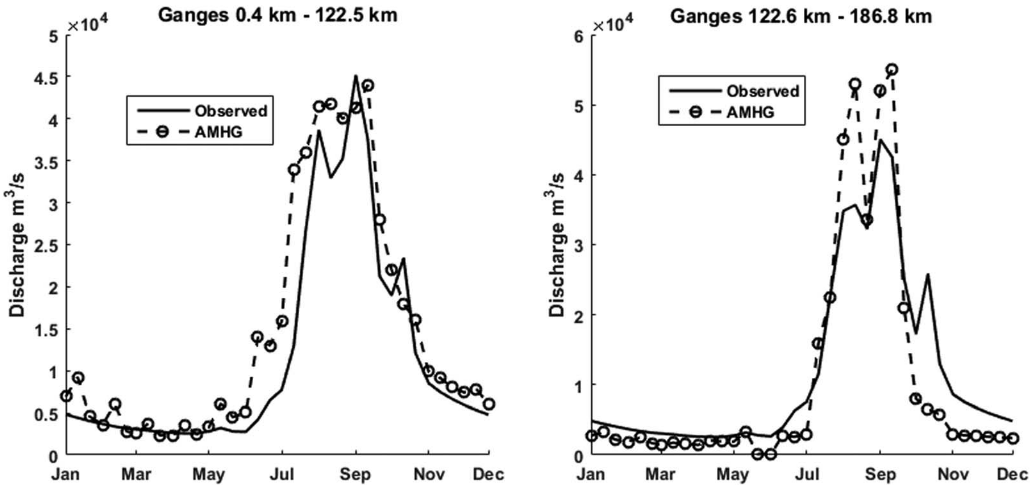

Figure 13. The AMHG algorithm performance using a priori AMHG knowledge from HEC RAS Model.

wet seasons was obtained from the river width proxy (equation (3)) and compared to the AMHG calculated directly from the HEC-RAS model widths and discharge that represent the river's true AMHG. Table 4 shows these AMHG parameters, as well as the R^2 statistic of the directly calculated AMHG as a measure for how tight the a-b relationship for the river is. The table also shows the percent difference between the proxy estimated AMHG and the directly calculated AMHG.

As can be seen in Table 4, the proxy incorrectly estimated the actual river AMHG for almost all of the river reaches. Furthermore, one of the only AMHG slopes estimated correctly, that of the Arial-Khan Wet 38.5–48.9 km, exhibited a very loose AMHG ($R^2 = 0.3$), which is indicative that the AMHG method may not perform well. The other fairly closely estimated proxy, Ganges Dry 0.4–122.5 km, resulted in more skillful results (54% RRMSE). However, the inaccurately estimated proxy for Ganges Dry 122.6–186.8 km resulted in lower uncertainties (39.8% RRMSE), the cause of which is unclear at this time. Nevertheless, the fact that the only reasonably accurate proxy estimate of AMHG resulted in one instance of the AMHG method accurately estimating discharge indicate that more accurate estimations of AMHG could lead to more successful applications of the AMHG method.

Thus, we tested a "corrective" approach on the Ganges River data. The Ganges River daily discharge and river width data from HEC-RAS for the year 2000 were used to obtain estimates of the AMHG parameters. This width and discharge data were the same data provided to the MFG algorithm for calibration and the Metropolis Manning algorithm for prior parameter estimation. These were fed into the AMHG method with the same width data from the study period of 2001. Figure 13 shows the results of this approach of relying on a priori model-based hydraulic parameters.

It is clear from Figure 13 that the AMHG discharge estimation accuracy is greatly improved for the Ganges River by using prior knowledge of the river's discharge. Table 5 shows the Ganges River error statistics using the corrective approach on AMHG values. This shows that the AMHG method can provide skillful discharge estimates with accuracies comparable to the MFG and Metropolis Manning algorithms, even during the wet

Table 5. Ganges River Error Statistics With Corrected AHMG Approach Relying on A Priori Information

	MFG		Metropolis Manning		AMHG	
	Dry	Wet	Dry	Wet	Dry	Wet
Ganges 0.4–122.5 km						
RMSE (m^3/s)	1592	5741	1361	6724	1703	6776
RRMSE (%)	48.4	34.4	41.4	40.3	51.8	40.5
Ganges 122.6–186.8 km						
RMSE (m^3/s)	1574	5384	1703	7082	1310	7869
RRMSE (%)	47.8	32.2	51.7	42.3	39.8	47.0

AGU Water Resources Research 10.1002/2015WR017296

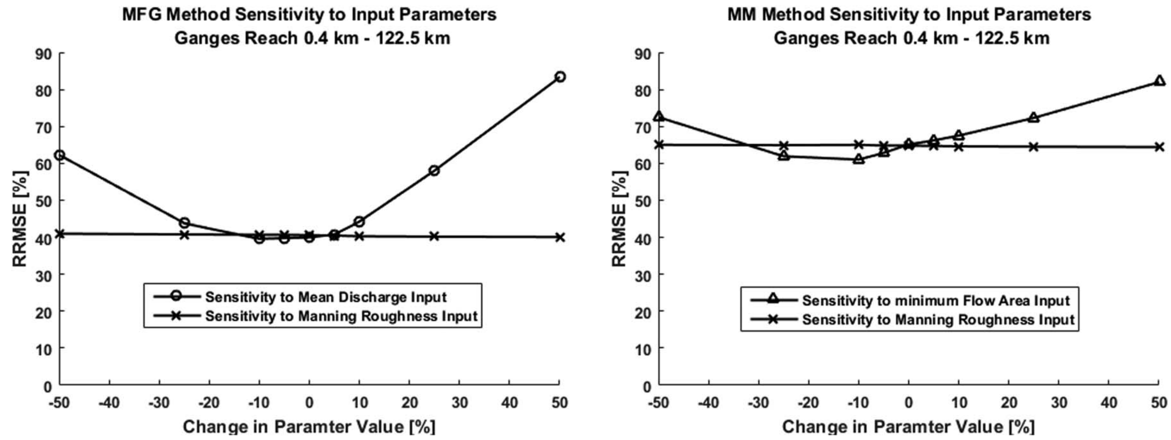

Figure 14. Algorithm sensitivities to change in input parameters for the Ganges reach 0.4–122.5 km of (left) the MFG method and (right) the Metropolis Manning method.

season. The dependence on the proxy is further confirmed with the good AMHG performance found by *Gleason and Hamdan* [2016] for the Ganges, where in their case they did not rely on the proxy but instead assumed an AMHG slope of −0.30, which agrees with observed data. Improving the performance of AMHG without use of a priori knowledge is a key challenge to the AMHG method and an area of active research: the AMHG method has limited utility for the rivers studied here without further refinement.

4.5. Sensitivity to Algorithm Input Parameters

The Metropolis Manning and MFG methods both require a priori information in order to estimate discharge. The Metropolis Manning method requires estimates for the Manning's roughness parameter as well as an estimate of cross-sectional area under minimum flow conditions. The MFG method also requires an estimate of Manning's roughness as well as the average discharge of the river. Here we tested the sensitivity of the estimated discharge from both algorithms to these input parameters. Each algorithm was run multiple times while varying these input parameters by modifying the original value (i.e., the parameter values used to generate the results in sections 4.1–4.3) by ±5%, ±10%, ±25%, and ±50%. Only one parameter was modified at a time and the sensitivities of the methods to changing more than one parameter at one time were not evaluated.

The results of the sensitivity analysis are shown in Figure 14. For clarity, only the results from the Ganges reach 0.4–122.5 km are shown. The trends shown here are representative of the algorithm sensitivities on all reaches. Figure 14 shows that the MFG method is not sensitive to changes in the input Manning's roughness parameter, with RRMSE remaining at a constant 40% for all tested values. The MFG method was sensitive to the input mean discharge, with RRMSE ranging from 39% at −10% of the original input value to 79% at +50% of the original input value. The Metropolis Manning method was also insensitive to changes in the input Manning's roughness parameter, with RRMSE remaining constant at 66% for all tested parameter values. The Metropolis Manning was sensitive to changes in the minimum flow area input, with RRMSE ranging from 62% at −10% of the original input value to 85% at +50% of the original value. For this reach, both methods appear to have a minimum error around −10% of the input parameters. On other reaches, this minimum error occurred at different changes in parameter values ranging from −25% to +10% and were not always in the same location for both algorithms (e.g., the minimum error for the second Ganges reach occurred at −25% for the MFG method, and at −10% for the Metropolis Manning method).

The sensitivity of both algorithms appears to be similar in magnitude. Both algorithms require a record of river observations in order to estimate the necessary input parameters. Repeated measurements of river cross-sectional area during a river's dry season are needed to estimate minimum flow for the Metropolis Manning method. At least a 1 year record of discharge estimates is required to accurately estimate a river's average discharge for the MFG method. This sensitivity analysis highlights the reliance of these two methods on good estimates for their input parameters, minimum flow area for the Metropolis Manning method, and mean discharge for the MFG method.

AGU Water Resources Research 10.1002/2015WR017296

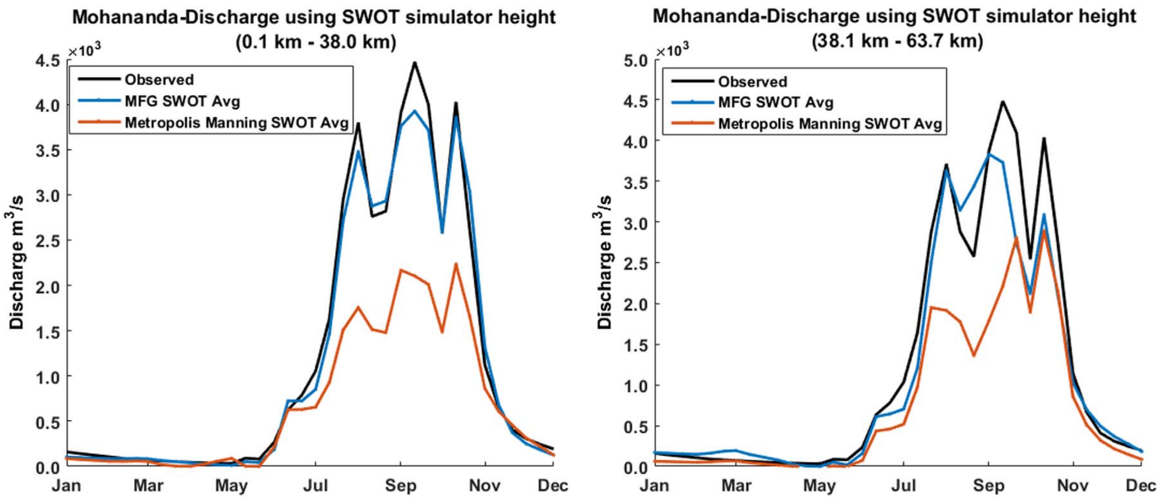

Figure 15. Mohananda River SWOT simulator-based algorithm results.

4.6. Implications for the Planned SWOT Mission

To gain a basic understanding of the implications of the above results for the SWOT mission, SWOT simulated river height observations of the 36 days in 2001 for the Mohananda River were run through the MFG and Metropolis Manning algorithms along with river widths obtained from the HEC-RAS model. As we had only considered the simulated height from the SWOT simulator (and not SWOT river widths) along with the true width (from HEC-RAS) of the river, the AMHG method's response to SWOT observables could not be tested.

The MFG and Metropolis Manning algorithms were applied using the river height and slope derived from SWOT simulator water level and the width data from the HEC-RAS simulation (the same data used in the previous section to test the algorithmic uncertainty) to calculate the discharge. Two sets of discharge were generated for each date, one by orbit-0261 output and another by orbit-0498 output. The average of these two sets is considered here as the discharge estimated from the SWOT simulator output. Figure 15 shows the observed and SWOT simulated algorithm discharge for the MFG and Metropolis Manning algorithms and Table 6 shows the corresponding error statistics.

Propagating remote sensing errors through the algorithms had two significant effects on discharge estimation accuracy. The MFG method in the second reach performed considerable less skillfully during the dry season (RRMSE increased by 15.3%). In contrast, the Metropolis Manning algorithm experienced a large increase in dry season accuracy in both reaches (RRMSE decreased by 19.4% and 83.2%). These accuracy increases could be the result of the SWOT simulated observations forcing the algorithm to search a wider range of parameter values to find the minimum error than the reference data. With the reference data, the Metropolis Manning algorithm could have converged to a local minimum and the introduction of SWOT errors could cause the algorithm to converge to a more optimal minimum. In all other cases, both algorithms performed only slightly worse

Table 6. Comparison of Algorithm Performance Between Discharge Estimations Using Reference River Observations and Discharge Estimations Using SWOT Simulated River Observations

		RMSE (m^3/s)		RRMSE (%)	
		Reference Observations	SWOT Simulated Observations	Reference Observations	SWOT Simulated Observations
0.1–38.0 km					
MFG	Dry	29	25	35.9	31.4
	Wet	197	205	10.5	10.9
MetroMan	Dry	66	51	81.7	62.3
	Wet	1049	1186	55.9	63.2
38.1–63.7 km					
MFG	Dry	47	60	58	73.3
	Wet	480	487	25.6	26
MetroMan	Dry	119	52	146.3	63.1
	Wet	1035	1036	55.2	55.3

AGU Water Resources Research 10.1002/2015WR017296

than with reference observations. These results indicate that the Metropolis Manning algorithm may be more sensitive to uncertainty in remotely sensed river surface elevation. This is most likely due to the unrealistic assumption of no observational uncertainty in river width, which at the time of writing this manuscript, a proper procedure to rationalize extraction of SWOT-river widths from the simulator was absent.

It should be noted that the minimum or zero flow stage in the MFG algorithm is analogous to the minimum flow area in the Metropolis Manning algorithm. Thus, the convergence of the MFG and Metropolis algorithms might be used as an additional objective function for optimizing the discharge estimation. Additionally, the AMHG could be used to derive a mean discharge as a function of width based on general regime theory [*Leopold et al.*, 1964] and used to calibrate the MFG zero flow depth and the Metropolis Manning minimum cross-section area. These considerations point to the advantage for synergistic application of multiple algorithms as a "team."

An important consideration for application of the algorithms is the reach length over which the slope should be derived, and which average values of width and stage should be assessed. In most cases, this length may be determined from observational data limitations, but in a best case scenario, should be related to a reach length that encompasses repeating geomorphic channel features such as a meander length, or a repeating braiding or multichannel pattern, or riffle pool sequence.

5. Conclusion

This first tier of assessment of three discharge algorithms designed to work with data from the upcoming SWOT mission showed that the MFG and Metropolis Manning algorithms generally outperformed the AMHG algorithm. Both the MFG and Metropolis Manning algorithms provided the better performance on different reaches and seasons, with at least one of the two typically producing discharge estimates with less than 50% RRMSE. Furthermore, the study found that the AMHG method can be improved during the wet season using a priori information of discharge, and such improvement is needed for operational application of AMHG. The impact of SWOT estimation uncertainty of river height on discharge accuracy appeared insignificant. In general, the MFG method was found to remain relatively more accurate while the Metropolis Manning algorithm appeared more sensitive to SWOT height observation errors. However, the SWOT elevation errors estimated here were limited by excluding errors occurring outside the true water extent. Thus, the error simulated here is an underrepresentation of the overall errors expected from the SWOT mission. Future studies should further explore the effects of SWOT error on discharge estimation as more complete SWOT simulator packages become available.

Overall, the MFG algorithm appeared to be the most stable of the three discharge algorithms in the Ganges river system. However, its dependence on knowledge of prior mean river discharge and various hydraulic flow parameters (width and height) suggests that it is not suited for a completely ungauged river system lacking in historical records. For the vast majority of cases in the developing world, the Metropolis Manning or AMHG method may be the more practical alternative for using satellite water elevation data to estimate discharge. Furthermore, the fact that the Metropolis Manning algorithm and the MFG algorithm seemed to excel in different cases and the region-specific correction improved AMHG performance, a multialgorithm ensemble approach of algorithms working as a "team" may be the future of spaceborne discharge estimation.

Future studies need to look into how a multialgorithm ensemble can work under a given set of heuristics, in order to be assimilated or "merged" as a more robust estimate than the individual algorithms. The underlying heuristics of when to "switch" from one algorithm to another as a function of season or river reach may also be worth exploring. Going beyond an ensemble approach, the extent to which these methods can cooperate with each other should also be explored. Perhaps discharge derived from the AMHG method can serve as a basis for calibration of the MFG or Metropolis Manning methods. Finally, future studies should also explore how best to assimilate the satellite observations on height and width from nadir altimetry and SWOT mission in widely used hydrodynamic models such as HEC RAS (a 2-D version has been released in 2015). We hope to continue our work along this direction and report our findings in a future paper.

AGU Water Resources Research 10.1002/2015WR017296

Acknowledgments

The authors acknowledge the NASA Physical Oceanography program (NN13AD97G) and NASA SERVIR program (NNX12AM85AG) for supporting this work. The Institute of Water Modeling (Bangladesh) is gratefully acknowledged for their generous support with data acquisition and hydrodynamic modeling as part of a 5 year memorandum of understanding with the University of Washington's Department of Civil and Environmental Engineering. Dani Esteban and Eva Peral are gratefully acknowledged for providing the SWOT simulator package. Additional guidance from Tamlin Pavelsky and Ernesto Rodriguez are also gratefully acknowledged. Data on HEC-RAS and SWOT Simulator for Mohananda River are available on request to the corresponding author of the manuscript.

References

Ackerman, C. T. (2009), *HEC-GeoRAS GIS Tools for Support of HEC-RAS Using ArcGIS User's Mannual*, Version 4.2, U.S. Army Corps of Eng. Inst. for Water Resour. AQ4

Alsdorf, D. E., E. Rodriguez, and D. P. Lettenmaier (2007), Measuring surface water from space, *Rev. Geophys.*, *45*, RG2002, doi:10.1029/2006RG000197.

Alsdorf, D. E., N. M. Mognard, and D. P. Lettenmaier (2011), Remote sensing of surface water and recent developments in the SWOT mission, Abstract H21J-06 presented at 2011 Fall Meeting, AGU, San Francisco, Calif.

Bates, P. (2004), Remote sensing and flood inundation modelling, *Hydrol. Processes*, *18*, 2593–2597, doi:10.1002/hyp.5649.

Berthon, L., C. Biancamaria, N. Goutal, S. Ricci, and M. Durand (2014), Towards the estimation of reach-averaged discharge from SWOT data using Manning's equation derived algorithm. Application to the Garonne River between Tonneins-La Reole, paper presented at EGU General Assembly, Eur. Geosci. Union, Vienna.

Biancamaria, S., D. P. Lettenmaier, and T. M. Pavelsky (2015), The SWOT mission and capabilities for land hydrology, *Surv. Geophys.*, *37*, 307–337, doi:10.1007/s10712-015-9346-y.

Biemans, H., I. Haddeland, P. Kabat, F. Ludwig, R. W. A. Hutjes, J. Heinke, W. von Bloh, and D. Gerten (2011), Impact of reservoirs on river discharge and irrigation water supply during the 20th century, *Water Resour. Res.*, *47*, W03509, doi:10.1029/2009WR008929.

Birkett, C. M. (1998), Contribution of the TOPEX NASA Radar Altimeter to the global monitoring of large rivers and wetlands, *Water Resour. Res.*, *34*(5), 1223–1239, doi:10.1029/98WR00124.

Bjerklie, D. M., S. L. Dingman, C. J. Vorosmarty, C. H. Bolster, and R. G. Congalton (2003), Evaluating the potential for measuring river discharge from space, *J. Hydrol.*, *278*(1–4), 17–38, doi:10.1016/S0022-1694(03)00129-X.

Bjerklie, D. M., D. Moller, L. C. Smith, and S. L. Dingman (2005), Estimating discharge in rivers using remotely sensed hydraulic information, *J. Hydrol.*, *309*, 191–209, doi:10.1016/j.jhydrol.2004.11.022.

Bray, D. I. (1979), Estimating average velocity in gravel-bed rivers, *J. Hydraul. Div.*, *105*, 1103–1123. AQ5

Calmant, S., and F. Seyler (2006), Continental surface waters from satellite altimetry, *C. R. Geosci.*, *338*, 1113–1122, doi:10.1016/j.crte.2006.05.012.

Dingman, S. L., and D. M. Bjerklie (2005), Hydrological application of remote sensing: Surface fluxes and other derived variables—River discharge, in *Encyclopedia of Hydrological Sciences*, edited by M. G. Anderson, John Wiley, New York. AQ6

Durand, M., L.-L. Fu, D. P. Lettenmaier, D. E. Alsdorf, E. Rodriguez, and D. Esteban-Fernandez (2010), The Surface Water and Ocean Topography mission: Observing terrestrial surface water and oceanic submesoscale eddies, *Proc. IEEE*, *98*, 766–779, doi:10.1109/JPROC.2010.2043031.

Durand, M., J. Neal, E. Rodriguez, K. M. Andreadis, L. C. Smith, and Y. Yoon (2014), Estimating reach-averaged discharge for the river severn from measurements of river water surface elevation and slope, *J. Hydrol.*, *511*, 92–104, doi:10.1016/j.jhydrol.2013.12.050.

Dyurgerov, M., and M. Meier (2005), Glaciers and changing Earth system: A 2004 snapshot, *Occas. Pap. 58*, INSTAAR, Univ. of Colo. at Boulder, Boulder.

Fu, L., D. Alsdorf, R. Morrow, and E. Rodriguez (2012), *SWOT: The Surface Water and Ocean Topography Mission: Wide-Swath Altimetric Measurement of Water Elevation on Earth*, Jet Propul. Lab., Pasadena, Calif.

Gleason, C. J., and A. N. Hamdan (2016), Crossing the (watershed) divide: Satellite data and the changing politics of international river basinism, *Geogr. J.*, doi:10.1111/geoj.12155, in press.

Gleason, C. J., and L. C. Smith (2014), Toward global mapping of river discharge using satellite images and at-many-stations hydraulic geometry, *Proc. Natl. Acad. Sci. U. S. A.*, *111*(13), 4788–4791, doi:10.1073/pnas.1317606111.

Gleason, C. J., and J. Wang (2015), Theoretical basis for at-many-stations hydraulic geometry, *Geophys. Res. Lett.*, *42*, 7107–7114, doi:10.1002/2015GL064935.

Gleason, C. J., L. C. Smith, and J. Lee (2015), Retrieval of river discharge solely from satellite imagery and at-many-stations hydraulic geometry: Sensitivity to river form and optimization parameters, *Water Resour. Res.*, *50*, 9604–9619, doi:10.1002/2014WR016109.

Hossain, F., and N. Katiyar (2006), Improving flood forecasting in international river basins, *Eos Trans. AGU*, *87*(5), 49–50, doi:10.1029/2006EO050001.

Leopold, L., M. Wolman, and J. P. Miller (1964), *Fluvial Processes in Geomorphology*, W. H. Freeman, San Francisco, Calif.

Leopold, L. B., and T. Maddock Jr. (1953), The hydraulic geometry of stream channels and some physiographic implications, U.S. Geol. Surv. Prof. Pap., 252.

Maswood, M., and F. Hossain (2014), Advancing river modeling in ungauged river basins using remote sensing: The case of Ganges-Brahmaputra-Meghna Basins, *J. River Basin Manage.*, doi:10.1080/15715124.2015.1089250. AQ7

Pavelsky, T., and M. Durand (2012), Developing new algorithms for estimating river discharge from space, *Eos Trans. AGU*, *93*(45), 457, doi:10.1029/2012EO450006.

Pavelsky, T., M. Durand, K. M. Andreadis, R. E. Beighley, R. C. D. Paiva, G. H. Allen, and Z. F. Miller (2014), Assessing the potential global extent of SWOT river discharge observations, *J. Hydrol.*, *519*, 1516–1525, doi:10.1016/j.jhydrol.2014.08.044.

Pokhrel, Y., N. Hansaki, S. Koirala, J. Cho, P. Yeh, K. Hyungjun, S. Kanae, and T. Oki (2012a), Incorporating Anthropogenic water regulation modules into a land surface model, *J. Hydrometeorol.*, *13*, 255–269, doi:10.1175/JHM-D-11-013.1.

Pokhrel, Y., N. Hansaki, P. Yeh, T. Yamada, S. Kanae, and T. Oki (2012b), Model estimates of sea-level change due to anthropogenic impacts on terrestrial water storage, *Nat. Geosci.*, *5*, 389–392, doi:10.1038/ngeo1476.

Schumann, G., P. D. Bates, M. S. Horritt, P. Matgen, and F. Pappenberger (2009), Progress in integration of remote sensing–derived flood extent and stage data and hydraulic models, *Rev. Geophys.*, *47*, RG4001, doi:10.1029/2008RG000274.

Siddique-E-Akbor, A. H. M., F. Hossain, C. K. Shum, F. J. Turk, S. Tseng, and Y. Yi (2014), Satellite precipitation data driven hydrologic modeling for water resources management in the Ganges, Brahmaputra and Meghna Basins, *Earth Interactions*, *18*, 1–25, doi:10.1175/EI-D-14-0017.1.

Sikder, S., and F. Hossain (2014), Understanding the geophysical sources of uncertainty for satellite interferometric-based discharge estimation in river deltas: The case for Bangladesh, *IEEE J. Selec. Top. Appl. Earth Obs. Remote Sens.*, *8*, 523–538, doi:10.1109/JSTARS.2014.2326893.

U.S. Army Corps of Engineers, *HEC-GeoRAS. Computer Software, Version 10.2*, Hydraul. Eng. Cent. AQ8

Vörösmarty, C., et al. (2004), Humans transforming the global water system, *Eos Trans. AGU*, *85*(48), 509–514, doi:10.1029/2004EO480001.

AGU Water Resources Research 10.1002/2015WR017296

Vörösmarty, C. J., J. P. Ericson, S. L. Dingman, L. G. Ward, and M. Meybeck (2007), Future impacts of fresh water resource management: Sensitivity of coastal deltas, in *Water Quality and Sediment Behaviour of the Future: Predictions for the 21st Century*, vol. 314, pp. 231–238. AQ9

Vörösmarty, C. J., J. Syvitski, J. Day, A. De Sherbinin, L. Giosan, and C. Paola (2009), Battling to save the world's river deltas, *Bull. At. Sci.*, *65* (2), 31–43, doi:10.2968/065002005.

Zarfl, C., A. Lumsdon, J. Berlekamp, L. Tydecks, and K. Tockner (2014), A global boom in hydropower dam construction, *Aquat. Sci.*, *77*, 161–170, doi:10.1007/s00027-014-0377-0.